

EFFECT OF RHUBARB FREE ANTHRAQUINONES ON OBESITY IN RATS AND ITS POTENTIAL MECHANISM

GUIFANG ZHANG^a, HAIJIAO WANG^a, SAEED ULLAH KHATTAK^b, HUIJUAN LV^a, LIFANG WANG^a, XUEFENG LI^c, XIUXIA SUN^{a*}, YANBIN SHI^{a,d*} 

^aSchool of Pharmacy and State Key Laboratory of Applied Organic Chemistry, Lanzhou University-730000, China. ^bCentre of Biotechnology and Microbiology, University of Peshawar, Peshawar, Pakistan. ^cSchool of Basic Medical Sciences, Lanzhou University, Lanzhou-730000, China. ^dCollaborative Innovation Center for Northwestern Chinese Medicine, Lanzhou-730000 University, China
*Corresponding author: Yanbin Shi; *Email: shiyb@lzu.edu.cn

Received: 30 Aug 2023, Revised and Accepted: 01 Oct 2023

ABSTRACT

Objective: The study was to confirm the effect of rhubarb-free anthraquinones (RhA) on anti-obesity and preliminarily explore the possible mechanism of action of RhA.

Methods: The obesity model of rats was induced by a high-fat diet to evaluate the effect of RhA on weight reduction and their potential mechanism based on network pharmacology and molecular docking as well as Western blotting analysis.

Results: RhA significantly reduced body weight, lipid-body ratio and Lee's index of the obese model rats. The level of low-density lipoprotein cholesterol significantly was decreased, and the number of fat droplets and fat cells in the liver tissue of the obese model rats was significantly reduced after treatment. The anti-obesity-related core proteins mainly targeted by RhA were predicted as MAPK8, MAPK14 and CASP3. Aloe-emodin, rhein, emodin, chrysophanol, and physcion had high affinity with these proteins. The relative expression of CASP3 and MAPK8 in the obese model rats was increased at gene and proteins levels after treatment.

Conclusion: RhA had significant weight-reducing and blood lipid-lowering effect of obese rats, and they may mainly intervene in obesity by up-regulating the expression levels of MAPK8 and CASP3 protein involved in fat metabolism.

Keywords: Rhubarb free anthraquinones, Anti-obesity, Network pharmacology, Molecular docking, Mechanism of action

© 2023 The Authors. Published by Innovare Academic Sciences Pvt Ltd. This is an open access article under the CC BY license (<https://creativecommons.org/licenses/by/4.0/>) DOI: <https://dx.doi.org/10.22159/ijap.2023v15i6.49272>. Journal homepage: <https://innovareacademics.in/journals/index.php/ijap>

INTRODUCTION

Obesity is a common chronic metabolic disease which can cause various complications such as colorectal cancer, type 2 diabetes and psychological problems [1, 2]. According to WHO statistics, more than 1.9 billion adults (39 percent of the global population) were overweight, of which more than 650 million (13 percent) were obese [3]. Orlistat, *et al.* have been approved by the FDA for marketing, which do have a significant effect on obesity, but their adverse reactions cannot be ignored, such as abdominal pain, diarrhea, vomiting [4, 5]. Finding active ingredients with weight loss from plants is one of the strategies for safer anti-obese drugs.

Rhei Radix et Rhizoma (Rhubarb) is the dried root and rhizome of genus *Rheum* (*Polygonaceae*), which has been widely used as a traditional medicine for two thousand years in China and Asian countries [6]. Current studies have shown that rhubarb has many pharmacological activities, such as fecal softening, lipid regulating and anti-inflammatory effect so on [7, 8]. The extract of rhubarb has been made into different supplementary food in the prevention of obesity, and rhubarb-free anthraquinones (RhA) consisted of aloe-emodin, rhein, emodin, chrysophanol and physcion are the major components of rhubarb extract [9], which may be responsible for its anti-obesity effect [10, 11].

Network pharmacology uses the connections between nodes to build interconnected networks and analyzes diseases by analyzing the connections of complex networks to identify biological relationships and the mechanism of action of the candidate drugs [12] This method is consistent with the holistic view of the core theory of traditional Chinese medicine (TCM) or systems biology which emphasizes that precise treatment should be based on syndrome differentiation. Herbal medicines have complex medicinal components which correspond to multiple interrelated targets and extensive signaling pathways. Based on the similar methodology, more and more studies have begun to apply network pharmacology to provide more fundamental and scientific explanations for

functional components and their mechanism of action in TCM modernization research [13, 14].

In this study, the obesity model of rats was induced by high-fat diet intake, and the effect of RhA on rat weight reduction was investigated. The main ingredients of RhA against obesity and obesity-related targets were analyzed by network pharmacology method. The component-target network and the protein-protein interaction (PPI) network of the interaction between the potential targets of RhA in the treatment of obesity were constructed. Signaling pathways for biological function were then investigated using Gene Ontology (GO) analysis and Kyoto Encyclopedia of Genes and Genomes (KEGG) enrichment analysis. The proposed functional components and main targets were further verified using molecular docking. Finally, qPCR and Western blotting were applied to confirm the predicted target genes and proteins.

MATERIALS AND METHODS

Chemicals and materials

The dried radix et rhizoma of *Rheum tanguticum* (abbreviated as Rhei Radix et Rhizoma) was purchased from Gannan Baicao Biotechnology Development Co., Ltd, Gansu province of China, and identified by Professor Zhigang Yang, working in Lanzhou University. A voucher specimen (No. 9206021) was deposited in the Institute of Pharmacognosy, School of Pharmacy of Lanzhou University. Reference standards of aloe-emodin, rhein, emodin, chrysophanol, and physcion were purchased from the Chengdu PUSH Bio-Technology Limt. Co. Ltd. Methanol (HPLC grade) was obtained from Fisher Scientific Ltd. (Pittsburgh, USA). High-fat feed was purchased from Jiangsu Xietong Pharmaceutical Bio-engineering Co., Ltd. Corn starch, sodium citrate and talc powder were purchased from Tianjin Damao chemical reagent factory. Assay kits of total cholesterol (TC), triglycerides (TG), low-density lipoprotein cholesterol (LDL-C) and high-density lipoprotein cholesterol (HDL-C) were purchased from Nanjing Jiancheng

Bioengineering Institute, China. MAPK8, MAPK14, CASP3, β -actin antibodies and secondary antibodies were purchased from SAB Biotechnology Co., Ltd, USA.

Animals

Sprague-Dawley rats (male, 200±20 g) were supplied by the Experimental Animal Center of Lanzhou University (License No. of Laboratory Animal Use Permit: SYXK, 2018-0002 [Gansu], Lanzhou, China). Animal experiments were approved by the Animal Experimentation Ethics Committee (20200306), School of Pharmacy, Lanzhou University, and conducted in accordance with the European Community guidelines for laboratory animal use and care (86/609/EEC). All animals were undergone adaptive rearing for one week before animal experiments.

Extraction of rhubarb-free anthraquinones

The dried Rhei Radix et Rhizoma was powdered and immersed with 70% ethanol (1:8, w/v) for 6 h, then extracted twice at 70 °C with 2 h each time. The extract was concentrated using a vacuum rotary evaporation equipment to recover ethanol, and the residue was diluted with water then extracted twice with dichloromethane (1:1, v/v). The dichloromethane extract was dried to obtain RhA. The identification of chemical constituents and content determination of RhA have been carried out in our previous research [9].

Preparation of RhA granules

Oral drug delivery is a preferred route since it is the most accessible and most convenient for patients [15]. The dry RhA extract was ground into powder, which was evenly mixed with equal amount of pharmaceutical starch then made into soft clumps with 10% starch slurry and 1.0 % sodium carboxymethyl cellulose (CMC-Na) as adhesives. The soft clumps were extruded into granules through a 14-mesh sieve, and the granules were dried to obtain RhA granules.

Modeling of obese rats and RhA intervention

Rats were allowed free access to food and water during a one-week adaptation period, then randomly divided into three groups with seven rats per group. Namely, normal control group fed with common maintenance diet (NC), obese rat model control group fed with high fat food and auxiliary materials of RhA granules (OC) at 30 mg granules/ml, obese rat model administration group given with high-fat food and RhA granules (OA) at the same dose, once a day for four weeks. The criteria for modeling success was the weight of rats in the OC group significantly increased compared with the NC group, while that in the OA group significantly decreased compared with the OC group.

Effect of RhA on rat obesity

General indices

During animal experiments, food intake and body weight were recorded each day; neck circumference and abdominal circumference were measured per 10 d; percent of body weight was calculated according to the formula 1.

$$\text{Percent of body weight} = \frac{\text{Body weight of rats} \times 100\%}{\text{Initial body weight of rats}} \dots (1)$$

Lee's index and weight ratio

The rats were sacrificed by neck dislocation under anesthesia before the trials ended. The body length (the length from snout to anus) and body weight were measured. Lee's index was calculated according to formula 2. The above-sacrificed rats were dissected, and the peri-testicle fat and liver tissue were collected, soaked in normal saline and blotted to dry on filter paper. The weight ratio was calculated according to formulas 3

$$\text{Lee's index} = \frac{\text{Body weight}(\text{g})^{\frac{1}{3}} \times 10}{\text{Body length}(\text{mm})} \dots (2)$$

$$\text{Weight ratio} = \frac{\text{Mass of peritestic fat of rats} \times 100\%}{\text{Body weight of rats}} \dots (3)$$

Glucose tolerance analysis

The rats were intraperitoneally injected with 50% glucose injection (5 g/kg) on the day before the trials ended, and blood was collected

by the tail vein on the last day. The blood glucose concentration was measured to evaluate the glucose tolerance of the rats.

Blood lipid analysis

The rats were anesthetized by inhalation of ethyl ether on the day before the trials began and the 30th day after the modeling started. Blood was collected from the orbital venous plexus, stood still for 2 h, centrifuged at 4 °C, 3000 rpm for 15 min, and then blood lipid levels were separately determined using serum TC, TG, LDL-C, HDL-C assay kits.

Histopathology observation

The peritesticle fat and the liver samples were fixed with tissue fixatives, embedded in paraffin, and stained with Hematoxylin and Eosin (H and E) for microscopic observation.

Analysis of Network Pharmacology

Screening targets of RhA

The main active compounds of RhA were searched by TCMSP (<https://old.tcmisp-e.com/tcmisp.php>) and TCMIP (<http://www.tcmip.cn>) Bioavailability (OB) is the fraction of an oral administered drug that reaches systemic circulation. Drug likeness (DL) is the similarity between a chemical substance and a known drug [16, 17]. Filter settings for retrieval of pharmacokinetic data for each compound were OB ≥ 18% and drug-likeness DL ≥ 0.18. Based on the PubChem database, the structure of the retrieved main active compounds was verified, and the simplified molecular input line entry system (SMILES) structural formula of the small molecules of the compound was obtained. Then the reverse molecular docking was performed in the Swiss Target Prediction database, and potential targets with Probability > 0.8 were selected. Additionally, the drug target was predicted in the PharmMapper database, and the prediction result was integrated with the target predicted in the Swiss Target Prediction database. The repeated target was removed to obtain the target of the main active compound of RhA [18, 19].

Construction of active component-target network

Cytoscape is a network biology visualization and analysis application that visualizes molecular connections and biological processes [20-22]. In order to visualize and simplify the complex relationship between the main active compounds of RhA, potential targets and obesity, the network file of the relationship between the screened target and the compound was imported into Cytoscape 3.8.1 software, and their relationship was abstractly represented as a "component-target" network, with nodes representing the corresponding components or targets, and edges representing the relationship between nodes.

Screening for common targets

The Gene Cards database and Open Targets database were searched for obesity-related disease targets with the keyword "obesity". The obesity-related disease targets obtained from the above databases were intersected with those predicted by the Swiss Target Prediction and PharmMapper databases to obtain a common target for the treatment of obesity by RhA.

Construction of PPI network

The component target and the obesity-related disease target were uploaded online in the software Venny 2.1. The obtained intersection is their common targets, and the Venn diagram was made accordingly. In order to explore the interaction relationship between the potential targets of RhA in the treatment of obesity, the common targets were uploaded in the SRTING database, and the species were selected as "Homo sapiens" [23, 24]. PPI information was input into Cytoscape 3.8.1 for visualization, and a PPI network was constructed [25, 26]. Network Analyzer was used for topology analysis, analyzing Betweenness Centrality, Closeness Centrality and Degree value of each node in the network. All these parameters can embody the properties of nodes in an interactive network [27-29]. Based on these parameters, 20 core targets were selected for further study.

Analysis of GO enrichment and KEGG pathway

The DAVID database (<https://david.ncicrf.gov/>) was used to perform GO analysis and KEGG signaling pathway enrichment

analysis on the selected 20 core targets. GO analysis includes biological process (BP), cellular component (CC), molecular function (MF). KEGG enrichment analysis can be used to discover important signaling pathways involved in biological processes. Subsequently, the GO and KEGG data were uploaded to the Bioinformatics (<http://www.bioinformatics.com.cn/>) platform for visual analysis to explore the body's metabolic process and possible signal transduction pathways involved in the core target of RhA in the treatment of obesity and select the most relevant core target proteins [30].

Molecular docking analysis

Molecular docking is a theoretical simulation method commonly used in drug screening to study the interaction and recognition of receptors and ligands. Intermolecular interactions were studied and their binding modes and affinities were predicted by this method [31, 32]. The binding ability of the main components of RhA to the core protein predicted by network pharmacology was evaluated by molecular docking, and the steps were as follows: the five active components of RhA were searched in the Pubchem database; their 3D structures were downloaded, and the files were saved in "mol2" format. The core target proteins screened were searched in the RCSB PDB database; the appropriate protein 3D structure was downloaded and the structure file was saved as a "pdb" suffix. The 3D structures of the core target proteins and active ingredients were

imported into MAESTRO version 11.5, and the proteins were dehydrated and hydrogenated by "Protein preparation" to generate a small molecule conformation at pH 7.0±2. The active ingredients were pretreated by "Ligand preparation" and the active sites were determined by the "Receptor Grid Generation" kit. The "Ligand Docking" panel was used for molecular docking and the semi-flexible docking method was selected. Finally, for visualization, the composite PDB format file was imported using PyMol 2.5 [33].

Target gene and protein analysis

Quantitative RT-PCR

The peritesticular adipose tissue of rats was collected and stored at -80 °C, and RNA was extracted according to the instruction of the RNA extraction kit (Wuhan Sevier Biotechnology Co., LTD.). Then RNA samples with appropriate purity were selected for reverse transcription and amplification using Servicebio@RT First Stand cDNA Synthesis kit and 2X SYBR Green qPCR Master Mix kit (low ROX) (Wuhan Sevier Biotechnology Co., LTD.). In this experiment, β -actin was used as reference gene, MAPK8, MAPK14, and CASP3 as target genes, and the relative mRNA expression of target genes was determined by calculation and comparison by $2^{-\Delta\Delta CT}$ method [9]. The primers were designed and provided by Sangon Biotech (Shanghai) Co., Ltd (Shanghai, China), and the sequences are listed in table 1.

Table 1: Primer sequences

Lot No.	Oligo name	Primer sequence (5' to 3')
2601097647	MAPK8 F	TGGATTGGAGGAGCGAACTAAGAATG
2601097648	MAPK8 R	CATTGACAGACGGCGAAGAGACC
2601097649	MAPK14 F	GAACAACATCGTGAAGTGTGAGAAGC
2601097650	MAPK14 R	CCTGTGGATTATGTCAGCCGAGTG
2601097651	CASP3 F	GCTGGACTGCGGTATTGAGA
2601097652	CASP3 R	TAACCGGGTGGGTAGAGTA

Western blotting

The peritesticular adipose tissue collected from the rats was stored under -80 °C, and extracted according to the instruction of protein extraction kit, and then the protein concentration was determined by BCA method [34]. The samples were diluted in SDS-PAGE loading buffer at 100 °C for 5 min, subjected to SDS-polyacrylamide gel electrophoresis. After transfer to a polyvinylidene difluoride (PVDF) membrane, western blotting membranes were stripped, blocked, and incubated overnight at 4 °C with MAPK8 (1:2000), MAPK14 (1:3000), CASP3 (1:2000) and anti- β -actin (1:5000) antibodies. After washing with TBST, the membranes were incubated with HRP-conjugated goat anti-rabbit IgG secondary antibody for 1 h at ambient temperature and visualised using the super ECL detection reagent. Finally, the target protein bands were scanned using FUSION SOLO6S. EDGE (VILBER, France), and the gray scale was quantitated using Image J. The relative expression level of protein was calculated based on the formula 4.

$$\text{Protein level} = \frac{\text{The gray scale of each protein}}{\text{The gray scale of } \beta\text{-actin}} \dots\dots\dots (4)$$

Statistical analysis

The data were expressed as mean±standard deviation (SD) and statistically analyzed by one-way analysis of variance (ANOVA) if the data were normally distributed and had homogeneous variance, and the LSD method was used for multiple comparison. A P-value<0.05 was considered statistically significant, while P<0.01 was considered highly significant. *: p<0.05, **, p<0.01, compared with NC group; #: p<0.05, ##: p<0.01 compared with OC group. The image analysis was performed using GraphPad Prism v8.3.0 and/or Image J software.

RESULTS

Food intake and body weight

During the experiment, the food intake of rats was controlled to keep the caloric intake of rats in each group similar that was 4760

kcal/kg for high-fat diet and 3616 kcal/kg for normal maintenance diet. The food intake curve of rats is shown in fig. 1.

As can be seen in fig. 2, the percentage of body weight of the OC group was significantly greater than that of the NC group (p<0.05), while the percentage of body weight of the OA group was significantly smaller than that of the OC group (p<0.05), even lower than that of the NC group.

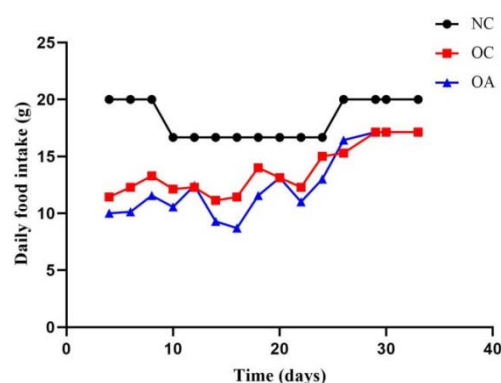


Fig. 1: Daily food intake of rats. (NC: normal control group; OC: obese rat model control group; OA: obese rat model administration group)

It can be seen in table 2, the neck circumference and abdominal circumference of the rats in the OC group were significantly greater than those in the NC group (p<0.05), while the neck circumference and abdominal circumference of the rats in the OA group were significantly less than those in the OC group (p<0.05).

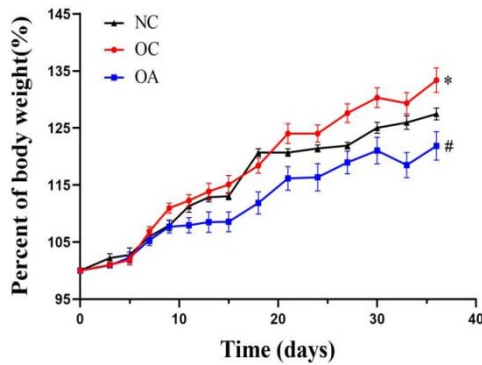


Fig. 2: Percent of body weight of rats in the different groups (NC: normal control group; OC: obese rat model control group; OA: obese rat model administration group; n=7, mean±SD)

Lee’s index and weight ratio

It can be seen from table 3 that after the last administration of the obese rats, the Lee’s index and weight ratio of the OC group were significantly greater than those of the NC group (p<0.05), while the Lee’s index and weight ratio in the OA group were significantly lower than those in the OC group (p<0.05).

Glucose tolerance and blood lipid levels

As shown in fig. 3, the blood glucose concentration of the rats in the OC group was significantly higher than that in the NC group at each period (p<0.05). Meanwhile, the blood glucose concentration of the rats in the OA group was lower than that of the OC group, and the blood glucose level at 1.5-2.0 h was almost the same as that of the NC group. The results indicated that the regulation of blood glucose of the OC rats was poor, while that of the OA rats was improved after RhA intervention.

Fig. 4 shows that the levels of LDL-C and TC in the OC group were significantly increased (p<0.05), while the level of HDL-C was significantly decreased (p<0.05) compared with the NC group. Notably, compared with the OC group, the LDL-C level of the OA group was significantly lower (p<0.05), suggesting that RhA may have a certain hepatoprotective effect.

H and E staining of rat adipose and liver tissue

The adipocytes in the NC group were uniform in size and stable in shape (fig. 5A), while those cells in the OC group were uneven in size, and some of them were very large (fig. 5B). Relatively, the adipocytes in the OA group were similar with those in the NC group in shape, regular in size, and tightly arranged (fig. 5C). In the liver slices, huge fat vacuoles appeared in the OC group (fig. 5E) compared with the liver in NC group (fig. 5D), while they were significantly reduced and became smaller in the OA group (fig. 5F).

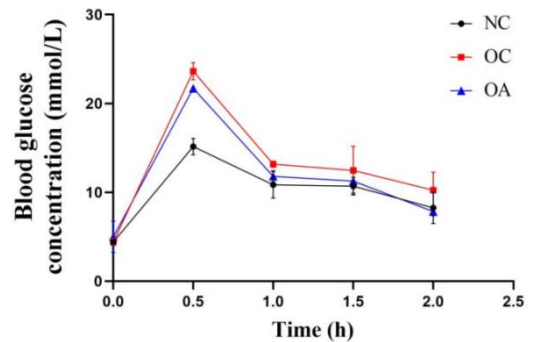


Fig. 3: Blood glucose level curve of rats after glucose administration (NC: normal control group; OC: obese rat model control group; OA: obese rat model administration group; n=7, mean±SD)

Table 2: Neck circumference and waist circumference of rats

Group	Neck circumference	Abdominal circumference
NC	10.38±0.26#	15.30±0.41#
OC	10.82±0.36*	15.87±0.46*
OA	10.37±0.28#	14.81±0.84#

Data are expressed as mean±SD, n=7

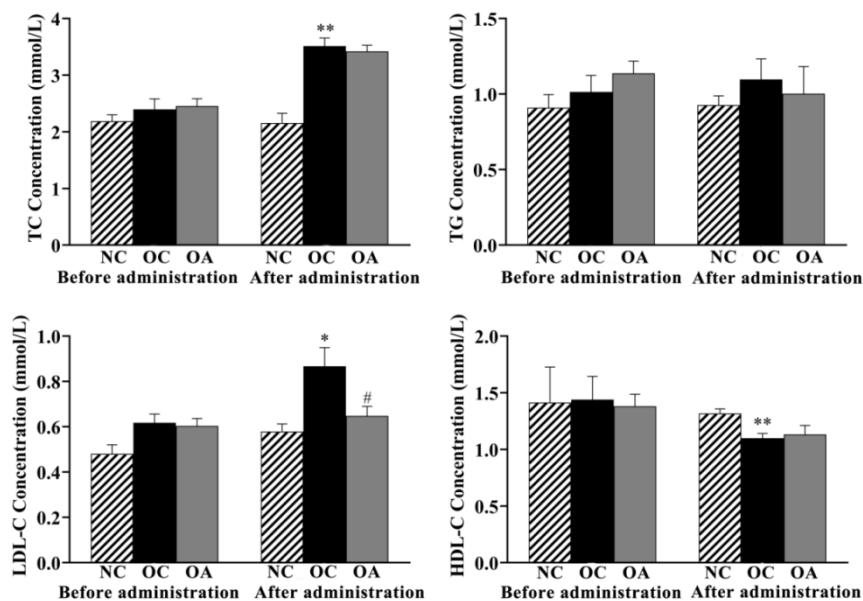


Fig. 4: Blood lipid levels in rats (NC: normal control group; OC: obese rat model control group; OA: obese rat model administration group; n=7, mean±SD)

Table 3: Lee's index and weight ratio of rats

Group	Lee's index	Weight ratio (%)
NC	0.306±0.004 [#]	1.05±0.03 [#]
OC	0.315±0.007 [*]	1.44±0.21 [*]
OA	0.307±0.006 [#]	1.14±0.28 [#]

Data are expressed as mean±SD, n=7

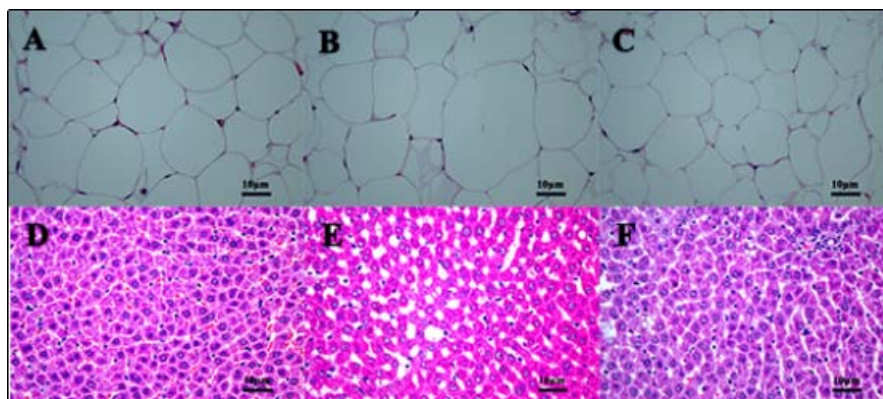


Fig. 5: H and E staining of adipose and liver tissues. A: Adipocytes of NC group; B: Adipocytes of OC group; C: Adipocytes of OA group; D: liver of NC group; E: liver OC group; F: liver of OA group (NC: normal control group; OC: obese rat model control group; OA: obese rat model administration group)

Compound-target network

As shown in fig. 6. There are 359 nodes (one drug ingredient-RhA, five RhA monomers including aloe-emodin, rhein, emodin, chrysophanol, physcion, and 353 corresponding targets) and 1424 edges in the diagraph. In the network, V-node represents drug ingredients, round nodes represent RhA monomers, and square nodes represent predicted potential targets corresponding to components. The edge connected between the nodes represents the relationship between RhA and the potential targets. Each potential target point corresponds to a variety of RhA compounds, indicating that RhA monomers may have multi-target and multi-component synergistic effect.

The main component information of five RhA monomers was retrieved, and the results are shown in table 4. The OBs were all greater than 18%, and the DLs were all greater than 0.20.

Considered comprehensively, all of them can be used as the main active components.

PPI network construction and analysis

As shown in fig. 7, a total of 9,496 obesity-related disease targets were retrieved, and 5,117 targets with a correlation score above the median were screened out, intersecting with the predicted 353 potential targets of the main compound of RhA. Finally, 208 common targets were obtained. The common targets were visualized and a PPI network diagram was constructed (fig. 8) which includes 205 nodes and 2379 edges. The round nodes represent the top 20 core targets. The edges connecting the nodes represent the interaction between common targets for the treatment of obesity by RhA and each target protein corresponds to many other target proteins, indicating that the target proteins are interrelated and cooperated to participate in the biological process *in vivo*.

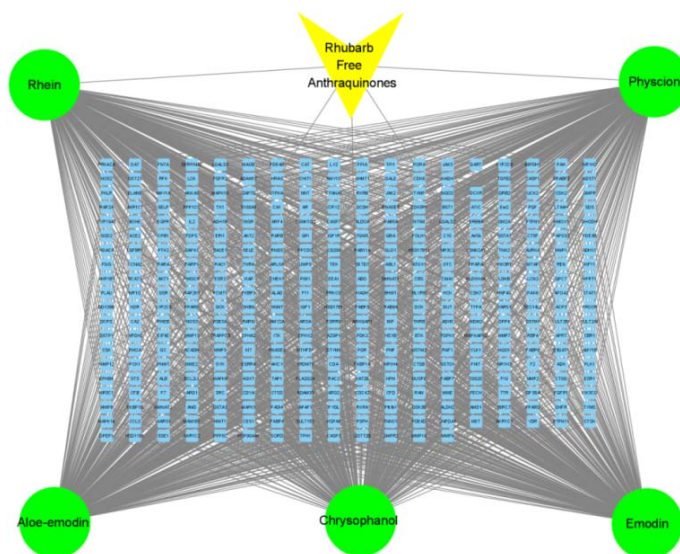
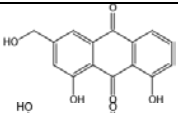
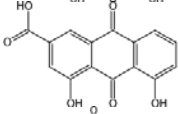
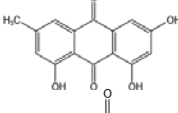
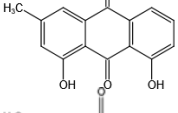
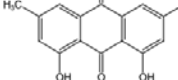


Fig. 6: Network diagram of rhubarb free anthraquinones-potential targets

Table 4: Information on five main components of RhA

No.	Structure	Compound name	Molecule ID	OB/%	DL
1		Aloe-emodin	MOL000471	83.38	0.24
2		Rhein	MOL002268	24.40	0.24
3		Emodin	MOL000472	47.07	0.28
4		Chrysophanol	MOL001729	18.64	0.21
5		Physcion	MOL000476	22.29	0.27

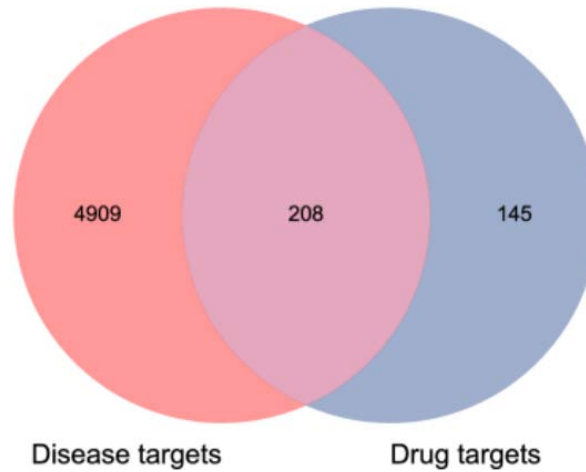


Fig. 7: Venn diagram of the intersection of RhA action targets and obesity disease targets

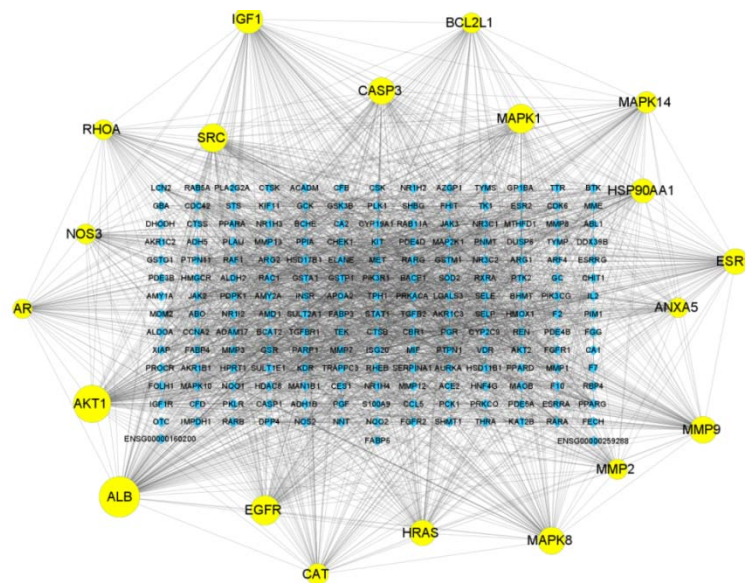


Fig. 8: The interaction network of target proteins of RhA in treating obesity, the topological analysis of the screened 20 core target proteins is shown in table 5, which was sorted according to the degree value

Table 5: Results of protein topological analysis of target protein of RhA in treating obesity

No.	Gene name	Protein name	Degree	Betweenness centrality	Closeness centrality
1	ALB	Albumin	123	0.177	0.711
2	AKT1	RAC-alpha serine/threonine-protein kinase	112	0.082	0.682
3	EGFR	Epidermal growth factor receptor	86	0.037	0.622
4	MAPK1	Mitogen-activated protein kinase 1	84	0.033	0.618
5	SRC	Proto-oncogene tyrosine-protein kinase Src	82	0.027	0.614
6	IGF1	Insulin-like growth factor I	81	0.027	0.613
7	MAPK8	Mitogen-activated protein kinase 8	78	0.019	0.605
8	MMP9	Matrix metalloproteinase-9	77	0.029	0.604
9	CASP3	Caspase-3	77	0.021	0.604
10	ESR1	Estrogen receptor	73	0.038	0.593
11	HRAS	GTPase HRas	73	0.016	0.598
12	HSP90AA1	Heat shock protein HSP 90-alpha	68	0.030	0.590
13	CAT	Catalase	60	0.046	0.576
14	MAPK14	Mitogen-activated protein kinase 14	59	0.011	0.565
15	MMP2	72 kDa type IV collagenase	55	0.010	0.560
16	BCL2L1	BCI-2-like protein 1	55	0.007	0.554
17	NOS3	Endothelial nitric oxide synthase	54	0.007	0.550
18	RHOA	Transforming protein RhoA	54	0.017	0.562
19	ANXA5	Annexin A5	53	0.007	0.559
20	AR	Androgen receptor	52	0.020	0.550

GO enrichment and KEGG pathway analysis

As shown in fig. 9, GO enrichment analysis showed that the BP mainly includes the response to reactive oxygen species, receptor tyrosine kinase, apoptosis signaling pathway, response to lipopolysaccharide, wound healing, mammary gland development and epithelial differentiation, regulation of exocytosis, ephrin receptor signaling, regulation of protein localization to membranes, protein kinase B signaling. CC mainly include vesicle lumens, focal adhesions, extrinsic components of plasma membranes, endocytic vesicles, cytoplasmic vesicle membranes, spindles, and collagen-

containing extracellular matrix. MF mainly includes nitric oxide synthase modulator activity, protein kinase binding, ATPase binding, heme binding, integrin binding, lipid binding, protein homodimerization activity, endopeptidase activity.

According to KEGG enrichment analysis (fig. 10), RhA mainly involves hsa01522 (endocrine resistance signaling pathway), hsa05200 (cancer pathway), ko05418 (fluid shear stress and atherosclerosis signaling pathway), ko04933 (AGE-RAGE signaling pathway in diabetic complications), hsa04912 (GnRH signaling pathway) and hsa05161 (hepatitis B signaling pathway) and so on.

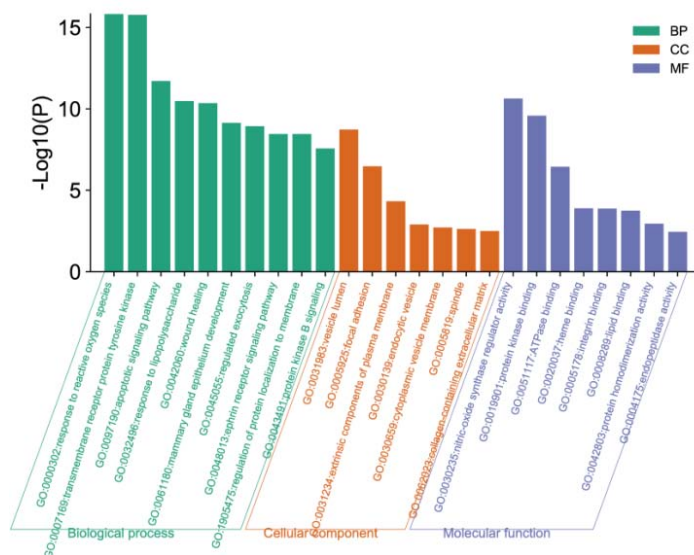


Fig. 9: GO enrichment analysis of the core target of RhA in treating obesity

The signaling pathways involved in the 20 core target proteins (table 6) demonstrated that MAPK8, MAPK14, and CASP3 proteins are respectively related to eight of the above-mentioned signaling pathways. Among them, six signaling pathways were consistent, namely hsa01522, ko04933, hsa04912, hsa05161, ko05145 (toxoplasmosis pathway) and hsa05120 (epithelial cell signaling pathway in *Helicobacter pylori* infection). Therefore, MAPK8, MAPK14, and CASP3 were the most representatives, and they were selected as the final core target proteins.

Molecular docking

A docking score of less than -4.25 indicates average binding ability, less than -5 indicates good binding ability, and less than -7 indicates strong binding ability [35, 36]. It can be seen in table 7, the docking scores were all less than -5, indicating that the five active compounds and the three core target proteins all had good binding abilities. Among which chrysophanol had the strongest binding ability to MAPK8 (docking scores: -7.874) and the weakest binding ability to CASP3 (docking scores: -5.391).

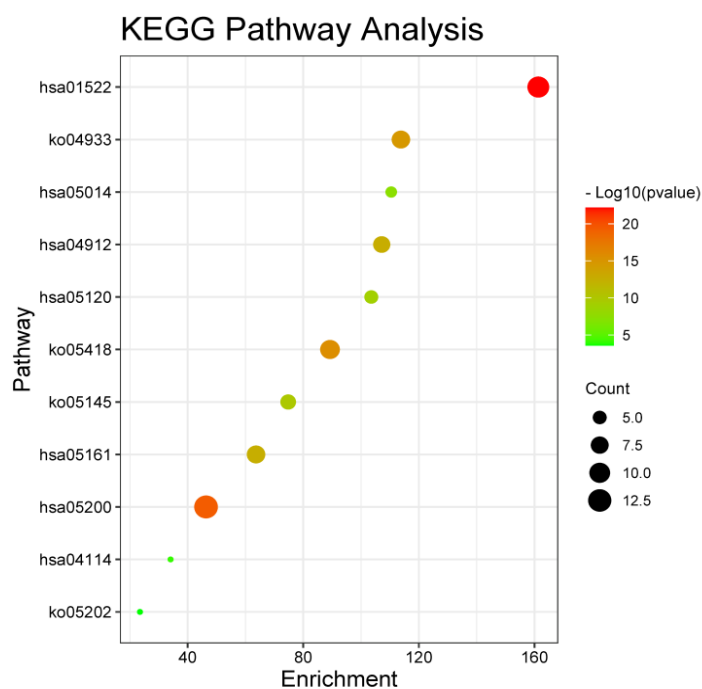


Fig. 10: KEGG enrichment analysis of the core target of RhA in treating obesity

Table 6: Signaling pathways involved in different target proteins

Mylist	hsa01522	hsa05200	ko05418	ko04933	hsa04912	hsa05161	ko05145	hsa05120	hsa05014	hsa04114	ko05202
ALB	0	0	0	0	0	0	0	0	0	0	0
AKT1	1	1	1	1	1	1	1	0	0	0	0
EGFR	1	1	0	1	1	0	1	1	0	0	0
MAPK1	1	1	0	1	1	1	1	0	0	1	0
SRC	1	0	1	1	1	1	1	1	0	0	0
IGF1	1	1	0	1	0	1	0	1	0	1	1
MAPK8	1	1	1	1	1	1	1	1	0	0	0
MMP9	1	1	1	0	1	1	0	0	0	0	1
CASP3	1	1	0	1	1	1	1	1	1	0	0
ESR1	1	0	0	1	0	0	0	0	0	0	0
HRAS	1	1	0	1	1	1	1	0	0	0	0
HSP90AA1	1	1	1	1	0	1	0	0	0	0	0
CAT	0	0	0	1	0	0	0	0	1	0	0
MAPK14	1	0	1	1	1	1	1	1	1	0	0
MMP2	1	1	1	1	1	0	0	0	0	0	0
BCL2L1	0	1	0	1	0	1	1	0	1	0	1
NOS3	1	0	1	1	1	0	1	0	0	0	0
RHOA	1	1	1	1	1	1	0	1	0	0	0
ANXA5	0	0	0	0	0	0	0	0	0	0	0
AR	0	1	0	1	0	0	0	0	0	1	0

Table 7: Molecular docking results of the active components and core targets of RhA

Target protein	PDB ID	Small molecule compound	Docking score
MAPK8	4L7F	Aloe-emodin	-7.499
MAPK8	4L7F	Rhein	-7.382
MAPK8	4L7F	Emodin	-7.583
MAPK8	4L7F	Chrysophanol	-7.874
MAPK8	4L7F	Physcion	-7.305
MAPK14	1OZ1	Aloe-emodin	-6.439
MAPK14	1OZ1	Rhein	-7.068
MAPK14	1OZ1	Emodin	-6.369
MAPK14	1OZ1	Chrysophanol	-6.577
MAPK14	1OZ1	Physcion	-6.501
CASP3	2J32	Aloe-emodin	-5.801
CASP3	2J32	Rhein	-6.119
CASP3	2J32	Emodin	-5.450
CASP3	2J32	Chrysophanol	-5.391
CASP3	2J32	Physcion	-5.868

Expression of the core target genes and proteins

Fig. 11 a and c show that the mRNA expression of MAPK 8 and CASP3 in peritesticular adipose tissue of the OC group was significantly decreased compared with the NC group ($p < 0.05$), while the mRNA expression of

MAPK 8 and CASP3 in peritesticular adipose tissue of the OA group was significantly increased compared with the OC group ($p < 0.05$). However, the mRNA expression of MAPK14 in the OC group was significantly higher compared with the NC group, and the mRNA expression of MAPK14 in OA group was significantly higher compared with the OC group ($p < 0.01$).

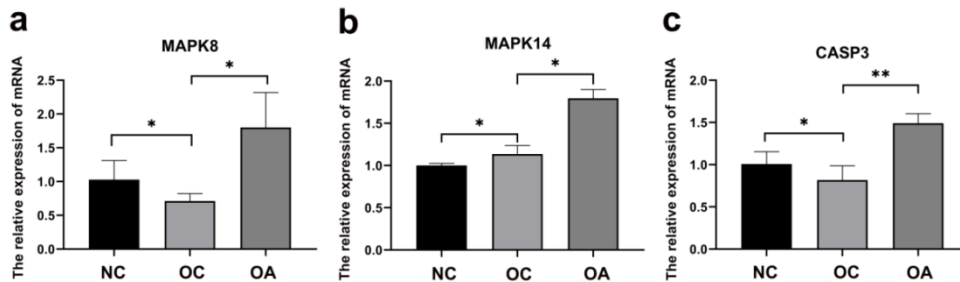


Fig. 11: The relative expression of MAPK8, MAPK14, CASP3 mRNA in peritesticular adipose tissue (NC: normal control group; OC: obese rat model control group; OA: obese rat model administration group; $n=3$, mean \pm SD)

According to fig. 12, the relative protein expression of CASP3 and MAPK8 in the OC group decreased compared with the NC group ($p < 0.05$), and those in the OA group increased compared with the OC

group ($p < 0.05$). The relative protein expression of MAPK14 in the OC group increased compared with the NC group ($p < 0.05$), and that in the OA group increased compared with the OC group ($p < 0.05$).

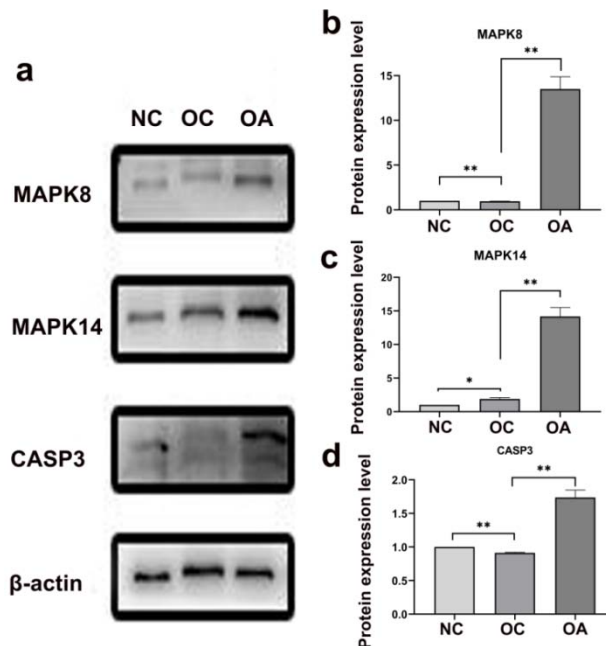


Fig. 12: The relative expression of MAPK8, MAPK14 and CASP3 proteins in fat tissue (NC: normal control group; OC: obese rat model control group; OA: obese rat model administration group; $n=3$, mean \pm SD)

DISCUSSION

Herbal products contain several active ingredients with varied or comparable pharmacological effects [37]. To better use the medicinal plant and improve their quality, research on potential active ingredients should be emphasized [38]. The main purpose of this study was to confirm the effect of RhA on anti-obesity and preliminarily explore the possible mechanism of action of RhA. Throughout the experiment, in order to avoid the influence of different food intake on the weight loss effect of the tested drug, each rat consumed as the same amount of calories as possible that was, the food intake of each rat was controlled as much as possible in a quantity. The calorie content of high-fat feed is 4760 kcal/kg, while the calorie content of normal feed is 3616 kcal/kg. The percentage of body weight of the OC group was significantly greater than that of the NC group, indicating obese rat modeling was successful. The percentage of body weight, neck circumference and

abdominal circumference, Lee's index, weight ratio of the OA group was significantly smaller than that of the OC group, suggesting that RhA can significantly slow down the body weight gain of rats. The results of H and E staining of rat adipose further supported the point. No obvious liver toxicity was observed based on pathological tissue section analysis, which was consistent with those reported [10]. The blood glucose concentration of the rats in the OC group was significantly higher than that in the NC group, and the intervention of RhA can effectively improve blood glucose level of the obese rats. Additionally, RhA could not change blood lipid levels except LDL-C in obese rats at the test dose. The result was inconsistent with the work we published before [9], possibly ascribed to different experimental doses and modelling method.

An ingredient-target network was constructed based on the characteristics of multi-component and multi-target of traditional Chinese medicine (TCM). Afterwards, a PPI network diagram was

constructed. Through network pharmacology analysis, five RhA monomers including aloe-emodin, rhein, emodin, chrysophanol were retrieved, and those five RhA monomers can act on multiple obese-related targets. Parts of the core targets, such as MAPK8, MAPK14, CASP3, were involved in multiple signaling pathways in the treatment of obesity. Among them, endocrine resistance signaling pathways are highly enriched which confers resistance to the most commonly used endocrine therapeutic agents (e. g., selective estrogen receptor modulators, estrogen synthesis inhibitors, and selective estrogen receptor down-regulators) through various mechanisms [39]. A lot of evidence showed that estrogen and estrogen receptors can lead to abnormal energy metabolism and energy imbalance, which may be one of the important factors affecting obesity [40, 41]. Therefore, we speculated that endocrine resistance signaling pathway were likely to be the main signaling pathways for RhA to treat obesity. A molecular docking score of less than -4.25 indicates average binding ability, less than -5 indicates good binding ability, and less than -7 indicates strong binding ability. The molecular docking results showed that five RhA monomers could be well bound to the three most correlated core target proteins of MAPK8, MAPK14, CASP3, and chrysophanol and MAPK8 had the lowest binding energy, indicating that the binding was the most stable [42].

Based on the prediction of network pharmacology, the expression of MAPK8, MAPK14, and CASP3 were investigated in obese rat peritesticular adipose tissue at both the gene and protein levels. The expressions of MAPK 8 and CASP3 in peritesticular adipose tissue of the OA group was significantly increased compared with the OC group, even higher than that of the NC group (fig. 11a and c and 12 a and c), indicating MAPK 8 and CASP3 were most likely targets of RhA, and RhA could effectively upregulate the expression of obesity-related genes to promote adipose metabolism in obese rats. On the contrary, the expression of MAPK14 of the OC group was significantly increased compared with the NC group, and that of OA group was significantly increased compared with the OC group (fig. 11b and 12 b), indicating RhA might lead to obesity in rats if the dose is given not enough. These results implied that RhA containing multi-components may bidirectionally regulate the expression of genes with different or even opposite function, resulting in synergistic and balanced effects on body metabolism. As expected, both genes and proteins expression analysis basically verified the possible anti-obesity mechanism of action of RhA predicted by network pharmacology. In a way, multi-component and multi-target based bidirectional regulation may be the unique benefit of plant medicine compared to single-component drug.

CONCLUSION

In this study, the effect of rhubarb free anthraquinones on anti-obesity was verified through *in vivo* animal experiments. MAPK8, MAPK14, and CASP3 were likely to be the targets of rhubarb free anthraquinones in the treatment of obesity, and they may mainly intervene in obesity through regulating endocrine resistance pathways closely related to fat metabolism by up-regulating the expression levels of MAPK8 and CASP3 proteins.

ACKNOWLEDGEMENTS

The work was financially supported by the Technology Innovation Guide Project of Gansu Province, China (22CX8NA002), the Lanzhou University Innovation and Entrepreneurship Cultivation Project (cxcy202114), the Medical Innovation and Development Project of Lanzhou University (lzuyxcx-2022-104), and the "Innovation Star" Project in 2023 of Lanzhou University (2023 cxzx-147).

FUNDING

Nil

AUTHORS CONTRIBUTIONS

Guifang Zhang: Methodology, Conceptualization, Writing-Original Draft. Haijiao Wang: Validation, Date analysis, Writing-Final Draft. Saeed Ullah Khattak: Writing-Review. Huijuan Lv: Investigation, Resources. Lifang Wang: Data Curation, Visualization. Xuefeng Li: Methodology, Validation. Xiuxia Sun: Conceptualization, Validation.

Yanbin Shi: Conceptualization, Writing-Review, Editing and Supervision.

CONFLICT OF INTERESTS

Declared none

REFERENCES

- Ethan L, Harold EB. Cancer and obesity: an obesity medicine association (OMA) clinical practice statement (CPS). *Obes Pillars*. 2022;3:100026. doi: 10.1016/j.obpill.2022.100.26.
- Zhang L, Wang Z, Wang X, Chen Z, Shao L, Tian Y. Prevalence of overweight and obesity in China: results from a cross-sectional study of 441 thousand adults, 2012-2015. *Obes Res Clin Pract*. 2020;14(2):119-26. doi: 10.1016/j.orcp.2020.02.005, PMID 32139330.
- Lee K, Kruper L, Dieli Conwright CM, Mortimer JE. The impact of obesity on breast cancer diagnosis and treatment. *Curr Oncol Rep*. 2019;21(5):41. doi: 10.1007/s11912-019-0787-1, PMID 30919143.
- Chaudhari D, Crisostomo C, Ganote C, Youngberg G. Acute oxalate nephropathy associated with orlistat: a case report with a review of the literature. *Case Rep Nephrol*. 2013;2013:124604. doi: 10.1155/2013/124604, PMID 24527242.
- Fujioka K. Safety and tolerability of medications approved for chronic weight management. *Obesity (Silver Spring)*. 2015;23Suppl 1:S7-11. doi: 10.1002/oby.21094, PMID 25900872.
- Zhang G, Li J, Lyu H, Qian C, Li X, Yang Z. Comparative pharmacokinetics of rhubarb anthraquinones loaded nanoemulsion by different plasma drug concentration calculation methods. *Acta Pol Pharm Drug Res*. 2021;78(4):475-83. doi: 10.32383/APPDR/141601.
- Huang H, Liu Z, Qi X, Gao N, Chang J, Yang M. Rhubarb granule promotes diethylnitrosamine-induced liver tumorigenesis by activating the oxidative branch of pentose phosphate pathway via G6PD in rats. *J Ethnopharmacol*. 2021;281:114479. doi: 10.1016/j.jep.2021.114479, PMID 34343647.
- Gao CC, Li GW, Wang TT, Gao L, Wang FF, Shang HW. Rhubarb extract relieves constipation by stimulating mucus production in the colon and altering the intestinal flora. *Biomed Pharmacother*. 2021;138:111479. doi: 10.1016/j.biopha.2021.111479, PMID 33774313.
- Wang Y, Zhang J, Xu Z, Zhang G, Lv H, Wang X. Identification and action mechanism of lipid regulating components from Rhei Radix et rhizoma. *J Ethnopharmacol*. 2022;292:115179. doi: 10.1016/j.jep.2022.115179, PMID 35278606.
- Fang JY, Huang TH, Chen WJ, Aljuffali IA, Hsu CY. Rhubarb hydroxyanthraquinones act as antiobesity agents to inhibit adipogenesis and enhance lipolysis. *Biomed Pharmacother*. 2022;146:112497. doi: 10.1016/j.biopha.2021.112497, PMID 34891117.
- Regnier M, Rastelli M, Morissette A, Suriano F, Le Roy T, Pilon G. Rhubarb supplementation prevents diet-induced obesity and diabetes in association with increased Akkermansia muciniphila in mice. *Nutrients*. 2020;12(10):2932. doi: 10.3390/nu12102932, PMID 32987923.
- Li S, Zhang B. Traditional Chinese medicine network pharmacology: theory, methodology and application. *Chin J Nat Med*. 2013;11(2):110-20. doi: 10.1016/S1875-5364(13)60037-0, PMID 23787177.
- Zhang R, Zhu X, Bai H, Ning K. Network pharmacology databases for traditional Chinese medicine: review and assessment. *Front Pharmacol*. 2019;10:123. doi: 10.3389/fphar.2019.00123, PMID 30846939.
- Fotis C, Antoranz A, Hatzivramidis D, Sakellaropoulos T, Alexopoulos LG. Network-based technologies for early drug discovery. *Drug Discov Today*. 2018;23(3):626-35. doi: 10.1016/j.drudis.2017.12.001, PMID 29294361.
- Agustina R, Setyaningsih D. Solid dispersion as a potential approach to improve dissolution and bioavailability of curcumin from turmeric (*curcuma longa* L.). *Int J App Pharm*. 2023;15:37-47. doi: 10.22159/ijap.2023v15i5.48295.

16. Ru J, Li P, Wang J, Zhou W, Li B, Huang C. TCMSp: a database of systems pharmacology for drug discovery from herbal medicines. *J Cheminform.* 2014;6:13. doi: 10.1186/1758-2946-6-13, PMID 24735618.
17. Shang J, Li Q, Jiang T, Bi L, Lu Y, Jiao J. Systems pharmacology, proteomics and *in vivo* studies identification of mechanisms of cerebral ischemia injury amelioration by Huanglian Jiedu decoction. *J Ethnopharmacol.* 2022;293:115244. doi: 10.1016/j.jep.2022.115244, PMID 35378193.
18. Qin T, Wu L, Hua Q, Song Z, Pan Y, Liu T. Prediction of the mechanisms of action of shenkang in chronic kidney disease: a network pharmacology study and experimental validation. *J Ethnopharmacol.* 2020;246:112128. doi: 10.1016/j.jep.2019.112128, PMID 31386888.
19. Tian S, Wang J, Li Y, Li D, Xu L, Hou T. The application of *in silico* drug-likeness predictions in pharmaceutical research. *Adv Drug Deliv Rev.* 2015;86:2-10. doi: 10.1016/j.addr.2015.01.009, PMID 25666163.
20. Kohl M, Wiese S, Warscheid B. Cytoscape: software for visualization and analysis of biological networks. *Methods Mol Biol.* 2011;696:291-303. doi: 10.1007/978-1-60761-987-1_18, PMID 21063955.
21. Wu L, Chen Y, Chen M, Yang Y, Che Z, Li Q. Application of network pharmacology and molecular docking to elucidate the potential mechanism of Astragalus-scorpion against prostate cancer. *Andrologia.* 2021;53(9):e14165. doi: 10.1111/and.14165, PMID 34185887.
22. Yeung N, Cline MS, Kuchinsky A, Smoot ME, Bader GD. Exploring biological networks with cytoscape software. *Curr Protoc Bioinformatics.* 2008;8:8.13.1-8.13.20. doi: 10.1002/0471250953.bi0813s23, PMID 18819078.
23. Szklarczyk D, Franceschini A, Kuhn M, Simonovic M, Roth A, Minguez P. The STRING database in 2011: functional interaction networks of proteins, globally integrated and scored. *Nucleic Acids Res.* 2011;39:D561-8. doi: 10.1093/nar/gkq973, PMID 21045058.
24. Szklarczyk D, Gable AL, Lyon D, Junge A, Wyder S, Huerta Cepas J. STRING v11: protein-protein association networks with increased coverage, supporting functional discovery in genome-wide experimental datasets. *Nucleic Acids Res.* 2019;47(D1):D607-D613. doi: 10.1093/nar/gky1131, PMID 30476243.
25. Zhang YL, Yin Q, Peng HM, Huang R, Zhou JW, Liu LH. Network pharmacology analysis and experimental validation to explore the mechanism of Hanchuan Zupa Granule in asthma. *J Ethnopharmacol.* 2021;281:114534. doi: 10.1016/j.jep.2021.114534, PMID 34419609.
26. Dong Y, Zhao Q, Wang Y. Network pharmacology-based investigation of potential targets of astragalus membranaceous-angelica sinensis compound acting on diabetic nephropathy. *Sci Rep.* 2021;11(1):19496. doi: 10.1038/s41598-021-98925-6, PMID 34593896.
27. Wang X, He Q, Chen Q, Xue B, Wang J, Wang T. Network pharmacology combined with metabolomics to study the mechanism of Shenyan Kangfu Tablets in the treatment of diabetic nephropathy. *J Ethnopharmacol.* 2021;270:113817. doi: 10.1016/j.jep.2021.113817, PMID 33444720.
28. Duan C, Li Y, Dong X, Xu W, Ma Y. Network pharmacology and reverse molecular docking-based prediction of the molecular targets and pathways for avicularin against cancer. *Comb Chem High Throughput Screen.* 2019;22(1):4-12. doi: 10.2174/1386207322666190206163409, PMID 30727880.
29. Tong H, Yu M, Fei C, Ji D, Dong J, Su L. Bioactive constituents and the molecular mechanism of curcuma rhizoma in the treatment of primary dysmenorrhea based on network pharmacology and molecular docking. *Phytomedicine.* 2021;86:153558. doi: 10.1016/j.phymed.2021.153558, PMID 33866197.
30. Zhang L, Han L, Wang X, Wei Y, Zheng J, Zhao L. Exploring the mechanisms underlying the therapeutic effect of Salvia miltiorrhiza in diabetic nephropathy using network pharmacology and molecular docking. *Biosci Rep.* 2021;41(6). doi: 10.1042/BSR20203520, PMID 33634308.
31. Pinzi L, Rastelli G. Molecular docking: shifting paradigms in drug discovery. *Int J Mol Sci.* 2019;20(18):4331. doi: 10.3390/ijms20184331, PMID 31487867.
32. Liu C, Liu J, Zheng Y, Qu J, Yang W, Tang X. Subchronic oral toxicity study of rhubarb extract in sprague-dawley rats. *Regul Toxicol Pharmacol.* 2021;123:104921. doi: 10.1016/j.yrtph.2021.104921, PMID 33894279.
33. Li X, Wei S, Niu S, Ma X, Li H, Jing M. Network pharmacology prediction and molecular docking-based strategy to explore the potential mechanism of Huanglian Jiedu Decoction against sepsis. *Comput Biol Med.* 2022;144:105389. doi: 10.1016/j.combiomed.2022.105389, PMID 35303581.
34. Xie Y, Shao R, Lin Y, Wang C, Tan Y, Xie W. Improved therapeutic efficiency against obesity through transdermal drug delivery using microneedle arrays. *Pharmaceutics.* 2021;13(6):827. doi: 10.3390/pharmaceutics13060827, PMID 34199630.
35. Yuan C, Wang MH, Wang F, Chen PY, Ke XG, Yu B. Network pharmacology and molecular docking reveal the mechanism of scopoletin against non-small cell lung cancer. *Life Sci.* 2021;270:119105. doi: 10.1016/j.lfs.2021.119105, PMID 33497736.
36. Cui Q, Zhang YL, Ma YH, Yu HY, Zhao XZ, Zhang LH. A network pharmacology approach to investigate the mechanism of Shuxuening injection in the treatment of ischemic stroke. *J Ethnopharmacol.* 2020;257:112891. doi: 10.1016/j.jep.2020.112891, PMID 32315738.
37. Sandopa D, Vellapandian C. Potential herb-drug interaction of decalepis hamiltonii via P-GP mediated pharmacokinetic interaction with fexofenadine in rats: an *in situ* and *in vivo* study. *Int J App Pharm.* 2023;15(5):128-33. doi: 10.22159/ijap.2023v15i5.48677.
38. Nounagnon MS, Dah Nouvlessounon D, N'Tcha C, Legba B, Baba Moussa F, Adjanohoun A. Phytochemistry and biological activities of *Crateva adansonii* extracts. *Int J Pharm Pharm Sci.* 2018;10(9):62-7. doi: 10.22159/ijpps.2018v10i9.27197.
39. Fan W, Chang J, Fu P. Endocrine therapy resistance in breast cancer: current status, possible mechanisms and overcoming strategies. *Future Med Chem.* 2015;7(12):1511-9. doi: 10.4155/fmc.15.93, PMID 26306654.
40. Chen JQ, Brown TR, Russo J. Regulation of energy metabolism pathways by estrogens and estrogenic chemicals and potential implications in obesity associated with increased exposure to endocrine disruptors. *Biochim Biophys Acta.* 2009;1793(7):1128-43. doi: 10.1016/j.bbamcr.2009.03.009, PMID 19348861.
41. Gerard C, Brown KA. Obesity and breast cancer-role of estrogens and the molecular underpinnings of aromatase regulation in breast adipose tissue. *Mol Cell Endocrinol.* 2018;466:15-30. doi: 10.1016/j.mce.2017.09.014, PMID 28919302.
42. Nasrin S, Islam MN, Tayab MA, Nasrin MS, Siddique MAB, Emran TB. Chemical profiles and pharmacological insights of *Anisomeles indica* Kuntze: an experimental chemico-biological interaction. *Biomed Pharmacother.* 2022;149:112842. doi: 10.1016/j.biopha.2022.112842, PMID 35325851.